Chapter 5
Sinter Plant Operations: Hazardous Emissions

Jin-Luh Mou and R. John Morrison

Abstract This article presents an outline of the iron ore sintering process, which introduces the blast furnace slag-forming requirements to allow an understanding of the required adjustments to flux addition in the sintering process; some basic concepts of the sintering reactions are also introduced. The recovery of miscellaneous wastes using high S, N, Cl content materials in sinter plants has been associated with some hazardous emissions, such as dust, NOx, SOx, and dioxins. The formation mechanism of these hazardous pollutants and some practical countermeasures are discussed.

5.1 Introduction

Before introducing the iron ore sintering process, some essential background information should be understood. This includes the following questions: why should iron ore fines be converted into lumpy materials? Why are fluxes added to the process? What are the chemical, physical, and metallurgical requirements of sinter ore?

The blast furnace operation is a bit like a black box; the gases and material flows interact counter-currently, and it is not possible to tell whether the iron burden is softening, melting, and dripping optimally inside the furnace. Only by checking the slag composition is it possible to tell whether the blast furnace is functioning satisfactorily or not.

A trigonal phase diagram of $CaO\text{-}SiO_2\text{-}Al_2O_3$ (Fig. 5.1) is an important guideline for blast furnace operations; accordingly, it is used to adjust the slag component ratio to reach near the eutectic point. This leads to the formation of the blast furnace slag with the lowest melting point, the best fluidity, and the best sulfur removal efficiency. Another important slag-forming component is MgO, which will facilitate the breaking of the slag silicate texture from framework, chain or double chain silicates into orthosilicates, or short-range silicates that enhances the fluidity.

J.-L. Mou
Formosa Ha-Tinh Steel Corporation, Ha-Tinh, Vietnam
e-mail: jinluhmou@gmail.com

R.J. Morrison (✉)
School of Earth and Environmental Sciences, University of Wollongong,
Wollongong, NSW, Australia
e-mail: johnm@uow.edu.au

P. Cavaliere (ed.), *Ironmaking and Steelmaking Processes*,
DOI 10.1007/978-3-319-39529-6_5

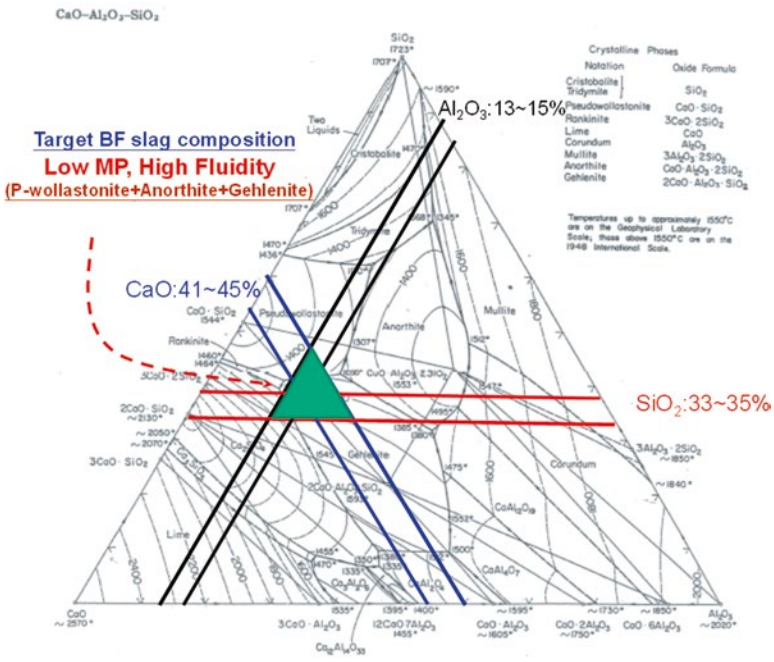

Fig. 5.1 Target BF slag composition based on the CaO-SiO_2-Al_2O_3 phase diagram

For the four major slag components, certain ratio ranges are required: $B_2 = CaO/SiO_2 = 1.15–1.25$, $B_3 = (CaO + MgO)/SiO_2 = 1.40–1.45$, and $B_4 = (CaO + MgO)/(SiO_2 + Al_2O_3) = 1.00–1.10$.

5.1.1 Size Requirements

A blast furnace is a "picky eater"; only the lumpy materials are fed into its belly. The size requirements of the iron burden for a blast furnace are iron ore lump, 6.3–31.5 mm; pellet, 9–18 mm; sinter, 5–50 mm; and coke, 25–80 mm. Iron ore fines, with the particle size of <10 mm, are not suitable as blast furnace feed. Several agglomeration processes have therefore been developed; if the ore type contains predominantly very fine particles (<0.075 mm), then a hot bond pelletizing process is applied. If the ore type has iron ore fines with coarser particles, then a sintering process is used.

5.1.2 Metallurgical Property Requirements

When the materials descend inside the furnace and the temperature reaches around 550 °C, Fe_2O_3 is reduced to Fe_3O_4 with around a 4 % volume expansion; some of the particles break down into small fragments and get blown out of the furnace with the

blast current. The breakage material is mainly composed of secondary hematite (the hematite that recrystallizes from the melt), therefore, to control the combustion atmosphere (to control the FeO level in sinter), and the chemical composition of sintering materials has become the key issue to minimize the reduction degradation.

When the temperature reaches 900–950 °C, magnetite (Fe_3O_4) is reduced to wustite (FeO); if the sinter has a compact texture without pores, then the reduction speed is low, and this reduces the burden descent speed, which leads to low BF productivity. The reducibility index is controlled mainly by the pore texture and is an important index for sinter ore.

When the temperature reaches 1400–1650 °C, the iron burden turns into liquid FeO or liquid Fe^0; softening and dripping occur in the cohesive zone. If the dripping melt has a high viscosity, then a coarser cohesive zone will be generated and will reduce the gas permeability, eventually resulting in low utilization of the reducing gas, and decrease the productivity. The softening and melting properties are controlled by slag components and the ratio among sinter, lump, and pellet; a good control of the burden ratio and slag-forming components is another important operational parameter.

5.2 Brief Background on Iron Ore Sintering

Modern sinter plants were developed in 1906 by Arthur S. Dwight and Richard L. Lloyd, and a chain grate strand type sinter machine which was able to operate continuously had been put into operation at Birdboro, Pennsylvania, USA, in 1911 (Vegman et al. 2004). The sintering process gained popularity quickly around the 1950s as positive links were found between blast furnace performance and ferrous burden of the sinter ratio.

5.2.1 Outline of Sintering Operations

Iron ore sintering is an agglomeration process, which combines fine mineral particles into a porous mass by partial liquefaction caused by heat generated from coke breeze combustion; a flow diagram of the iron ore sintering process is shown in Fig. 5.2.

The chemistry of the raw materials is calculated to fit BF slag formation requirements; under this operational guideline, iron ores together with fluxes (limestone, dolomite, serpentine) and reverts (mill scale, flue dust BOF OG sludge, etc.) are blended in the blending yard and conveyed to the sinter plant proportioning silos, where the coke breeze, sinter plant return fines (SP/RF), and tuning fluxes are added and granulated through mixing drums to form a sinter mixture that is laid onto the sinter strand. Eventually, the coke breeze is ignited by an ignition furnace to provide the energy for sintering.

The CaO and MgO slag components do not coexist with iron ores and are added separately; therefore, CaO (such as limestone) and MgO (such as serpentine or dolomite) are mixed with iron ore fines as the sinter raw mix for the sintering

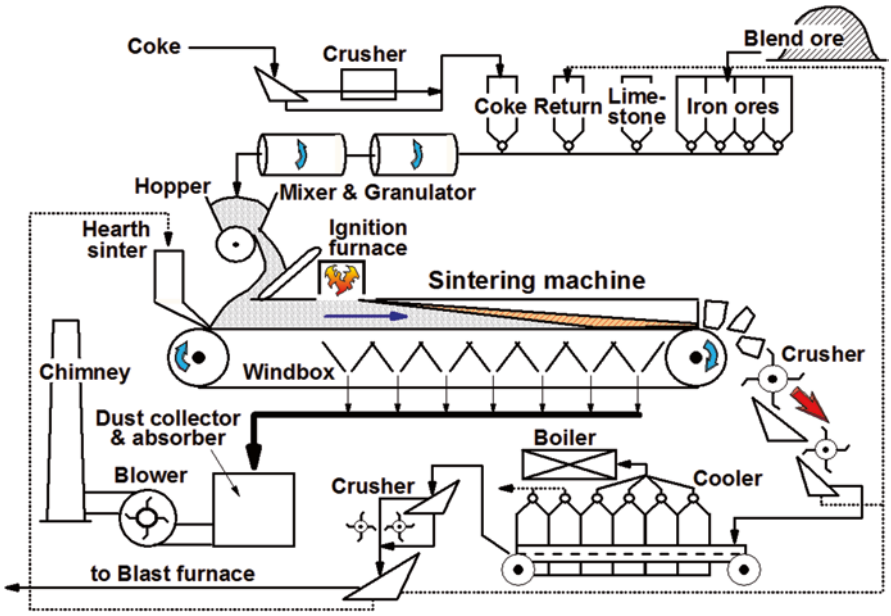

Fig. 5.2 Flow diagram of the iron ore sintering process

process. The ultrafine iron ore reacts with the fluxes and forms a bonding matrix (silico-ferrite of calcium and alumina, SFCA) at a reaction temperature of 1300 ± 50 °C from the combustion of coke breeze.

In order to promote the sinter plant productivity, a particle segregation device is installed to improve the sinter bed permeability. The main concept is to lay the coarse particles in the bottom layer and fine particles in the upper layer. There are several segregation devices, such as deflective plate, SSW (segregation slit wire, developed by Steel Plantech Corp.), ISF (intensified sifting feeder, developed by NSC), and MBF (magnetic braking feeder, developed by JFE).

Figure 5.3 shows a cross-sectional profile of sinter belt. The coke breeze is first ignited in the front end of the sinter strand; gas flow is sucked from upper surface and passes through the sinter bed to the bottom wind boxes. The combustion zone reaches the sinter bed bottom where sinter strand also reaches the tail end.

The inter-belt is thus classified into several regions; from the bottom part of the front end is a wet zone, where the moisture accumulates. A dry zone is found on top of the wet zone, as the moisture is driven down by the heat. On top of the dry zone are the coke breeze ignition and combustion zones, where the partial liquefaction occurs for sintering reaction. Cold gas is sucked in from the top surface and cools down the sinter cake in a cooling zone. After cooling, the sinter cake becomes brittle due to volume shrinkage. The wind box temperature is gradually increased from the front end to the tail and reaches the highest point, where the combustion zone reaches the bottom, and is called the burnt through point. The gas flow rate profile is similar to the temperature profile; the flow rate is higher in the tail end.

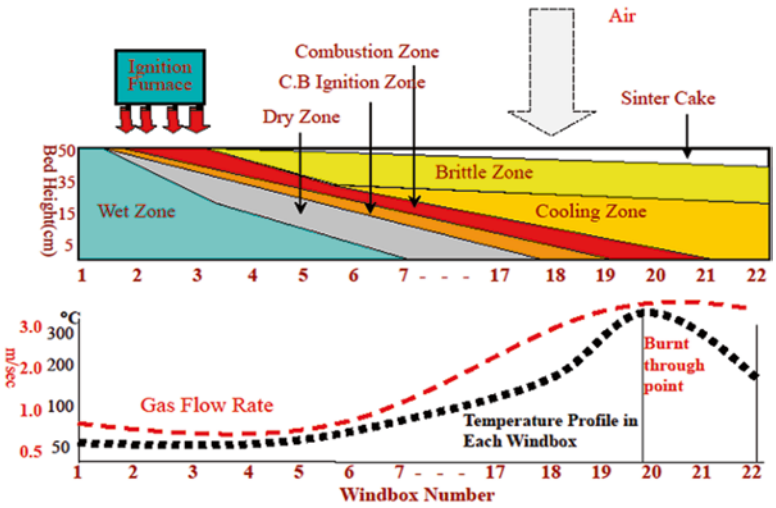

Fig. 5.3 Sinter belt cross section, temperature, and gas flow profiles in each wind box

5.2.2 *Fundamental Reactions of the Sintering Process (Pimenta 2012)*

In addition to the previous description of different temperature zones, a reduction region (rich in CO) is under the combustion zone, and an oxidation region, rich in O_2, is above the combustion zone. Below the material melting point, some reactions happen between solid-solid states, such as evaporation, dehydration, carbonate decomposition, reduction, or reoxidation.

The whole sintering process based on the heating stages can be split into five steps as shown in Fig. 5.4 (Pimenta 2012).

Step 1. Hematite (Fe_2O_3) reacts with CaO to generate the first calcium ferrites at around 1100 °C (solid–solid reaction). Around 1200 °C, these calcium ferrites start to convert into the liquid phase. The liquid is rich in CaO and Fe_2O_3 and begins to combine with ultrafine iron oxides, SiO_2, Al_2O_3, and MgO.

Step 2. Liquid phase starts to generate while temperature keeps on rising, and the superficial disintegration of hematite starts.

Step 3. The liquid melt assimilates with CaO and Al_2O_3, and the evolution of the reaction between liquid and hematite forms acicular calcium ferrites in the solid state (needle form), which are rich in Al_2O_3 and SiO_2.

Step 4. If the process temperature does not reach above 1300 °C or the residence time above 1300 °C is very short, the microstructure after cooling will be rich in acicular calcium ferrites in a bulk of crystalline silicates and granular hematite. That is the heterogeneous sinter.

Step 5. If the process temperature exceeds 1300 °C and the residence time above 1300 °C is long, columnar calcium ferrites and coarser recrystallized particles precipitate from melt. During the cooling step, skeletal rhombohedral hematite

precipitates from the liquid phase, and calcium ferrites crystallize as long columnar form flakes. That is the homogeneous sinter.

5.2.3 *Mineral Transformation During Iron Ore Sintering Process*

To convert the fine particles into lumpy agglomerates, the bonding matrix plays a major role (Fig. 5.5). When the coke breeze is combusted in the sinter bed, iron ore adhering fines together with the fluxes react and form the liquid melt; the wetting effect through this melt joins the iron ore particles together. Eventually, when the temperature cools down, this melt hardens, and the particles are bonded into lumpy

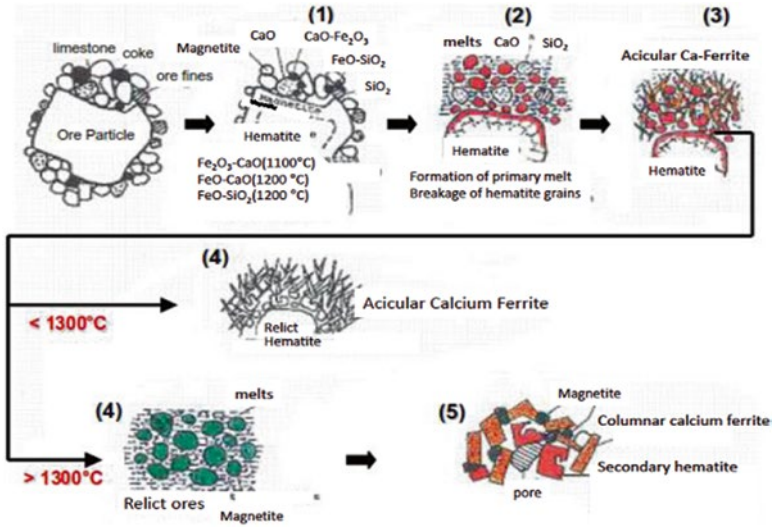

Fig. 5.4 Fundamental sintering process reactions

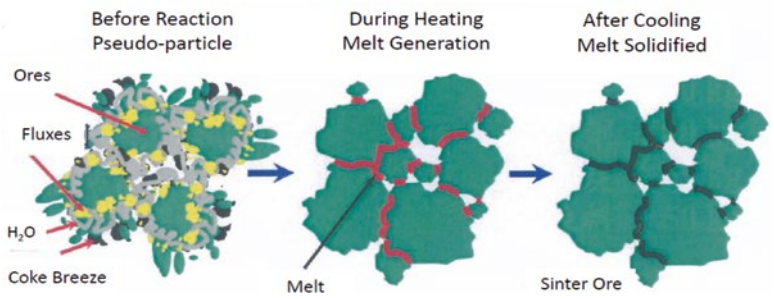

Fig. 5.5 Schematic diagram of the bonding matrix

agglomerate. Of course, dissolution, thermal decomposition, reduction, oxidation, recrystallization, etc., occur during the heating stage.

5.3 Hazardous Pollutant Emissions from Sinter Plants

Some of the hazardous elements, such as S and N, are brought into the process with the coke breeze or iron ores, and others, such as Pb, Zn, Na, K, S, Cl, and oil, may come from the revert materials. These unwelcome materials are brought into the system and are associated with the hazardous emissions. A sinter plant is the major pollutant source in an integrated steelworks; some estimated figures are summarized below, based on the assumed conditions.

Assumptions for a sinter plant emission:

An integrated steelworks produce 7.0 million tonnes of crude steel per annum (two sets of 4350 m^3 inner volume blast furnace), and the sinter ratio for the blast furnace is 80 %; then, two sets of 500 m^2 sinter plants are required to produce 10.2 million tonnes of sinter as the blast furnace iron burden. The fuel rate is 50 kg of coke breeze for per tonne of sinter, where the S content is 0.55–0.60 % and N is 0.8–1.0 % in the coke breeze. 2500 Nm^3 air is required to produce one tonne of sinter. Only a de-dusting electrostatic precipitator (EP) is installed, without installing the de-SOx, de-NOx, and de-DXNs devices. The estimated figures are as follows

O_2:	~15 %
CO:	8000–10,000 ppm
CO_2	5.0–6.0 %
Dust	40–50 mg/Nm^3
SOx	130–150 ppm
NOx	150–200 ppm
PCDD/PCDFs	0.8–2.0 ng I-TEQ/Nm^3

5.3.1 Dust

The off-gas dust concentration is about ~50 mg/Nm^3 with an EP removal efficiency of around 95 %; mostly the dust is composed of alkali chlorides and sulfates, which have high electric resistance and are hard to polarize in the electric field to be removed by the EP. These alkali chlorides are within the submicron particle range and generate the plume opacity together with the acid gases condensing on the surface as aerosols. A simple countermeasure is to install a multi-pulse type electric field generator and change the rapping frequency to clean the adhered particles off the electric plates and wires.

However, the most harmful PM2.5 is not monitored in the stack emissions. It has been assumed that PM2.5 forms 70 % of the PM10 measured in the waste gas (Wright 2014). This assumption is based on previous studies that have been undertaken by BlueScope Steel Limited that were considered as a reference index.

5.3.2 NOx (Mou 1998)

Suzuki et al. (1975) conducted sinter pot tests by replacing air with O_2(21 %) + Ar(79 %) and found no difference in the NOx emissions. This indicated that the NOx is fuel generated with almost no thermal NOx or prompt NOx in the sintering process.

An analysis of the chemical composition of the sinter raw materials showed that more than 90 % of the nitrogen comes from coke breeze (Mou 1992). It is difficult to identify what types of nitrogen compound exist in the coke breeze. However, it is believed that the nitrogen is tightly bound and for the most part in aromatic compounds. In the heating stage, the fuel-bound nitrogen compounds will, most likely, undergo some decomposition prior to entering the combustion zone; thus, it is not surprising that in the oxidation zone, the nitrogen compounds turn into the intermediates, such as HCN, CH, and amine radicals (Glassman 1987). These fragments react with oxygen in the continuous heating stage and form the nitrogen oxides. These intermediate compounds also contain hydrogen and carbon, which have a strong affinity with oxygen. In other words, the hydrogen or carbon will compete with nitrogen for the oxygen. Therefore, the presence C, CO, H, or OH in the combustion system will have some depression effect on the formation of nitrogen oxides.

Sasaki et al. (1990a, b) reported that a fast coke combustion rate led to higher $(CO + CO_2)/O_2$ and CO/O_2 ratio being found in the waste gases. Kasai et al. (1992) reported that faster coke combustion rate led to lower NO emissions. Obviously, the CO/O_2 ratio in the combustion zone is the major factor controlling the final NO emission. The combustion speed affects the atmospheric condition in the sintering process. Therefore, the improvement of coke combustibility would be a feasible countermeasure to depress the NO emission.

Not all the nitrogen content in the sinter raw mix would convert into nitrogen oxides in the sintering process; the conversion ratio will depend on the combustion condition especially the CO/O_2 ratio. Hida et al. (1980) and Kasai et al. (1992, 1993a, b) developed the conversion ratio formula. An estimated conversion ratio based on a real sinter plant operation data is around 36 % (Mou 1998).

5.3.3 De-NOx

Currently, there are less than five sets of de-NOx facilities being installed in the world sinter plants; the technique being applied is the SCR process. WO_3-TiO_2-V_2O_5 catalysts are applied for de-NOx operation, where the liquid NH_3 is injected into the reaction chamber under the operating temperature of 320–350 °C; the NOx removal efficiency can reach around 90 %. The reactions are summarized as follows.

$$4NO + 4NH_3 + O_2 \rightarrow 4N_2 + 6H_2O\,(\text{major reaction})$$

$$6NO + 4NH_3 \rightarrow 5N_2 + 6H_2O$$

$$2NO_2 + 4NH_4 + O_2 \rightarrow 3N_2 + 6H_2O$$

$$6NO_2 + 8NH_3 \rightarrow 7N_2 + 12H_2O$$

An in-process de-NOx study (Mou 1998) concluded that NOx emissions in iron ore sintering process depend mainly on the coke breeze combustion condition. A faster combustion speed results in lower NOx emission. To enhance the granulation and improve the permeability of the sinter mix has been shown to be an effective countermeasure by increasing the combustion speed and depressing the NOx emission.

This study also verified sugar is a strong binder in sinter mix granulation, improving sinter bed permeability and increasing the flame front speed; hence, the conversion ratio of nitrogen fragments to nitrogen oxides is greatly reduced. Sinter pot test results showed 1 wt% of sugar addition to the sinter mix decreased the NO mass from 533.8 to 283.3 g/t. sinter, with nearly 47 % NO mass reduction. The NOx concentration also decreased from 223 to 160 ppm with nearly 28 % concentration depression. Also, because of the shortened sintering time, sinter productivity is also significantly increased from 37.5 to 45.4 t/m^2/24 h as the sinter strength is maintained at the same level. Sugar is a potential additive for in-system de-NOx in the iron ore sintering process.

5.3.4 SOx

The sulfur compounds in the sinter mix may be in organic or inorganic forms. In iron ores, especially igneous magnetite, some pyrite (FeS_2) or chalcopyrite ($FeCuS_2$) is always present and difficult to get rid of through magnetic separation or washing processes. In coke breeze, there are either organic or inorganic sulfur compounds. Although in the coal washing process some of the pyrite can be removed through flotation and density separation, the removal efficiency is limited by the size of pyrite. It is very difficult to separate organic compounds from the coal. In the coking process, some of the sulfur compounds go into the by-products or escape to the atmosphere, and some others still remain in the coke, which is the major source of sulfur oxides in sintering.

SO_2 generated in the heating stage may be trapped by water (Martin 1984), limestone (Anderson and Galwey 1995), or iron ores (Tu and Liu 1992); SO_2 existing in water (referred to as S(IV)) occurs as three species, which are hydrated sulfur dioxide, bisulfite ion, and sulfite ion (Anderson and Galwey 1995).

$$\left[\mathrm{S(IV)}\right] = \left[SO_{2(aq)}\right] + \left[HSO_3^-\right] + \left[SO_3^{2-}\right] \tag{5.1}$$

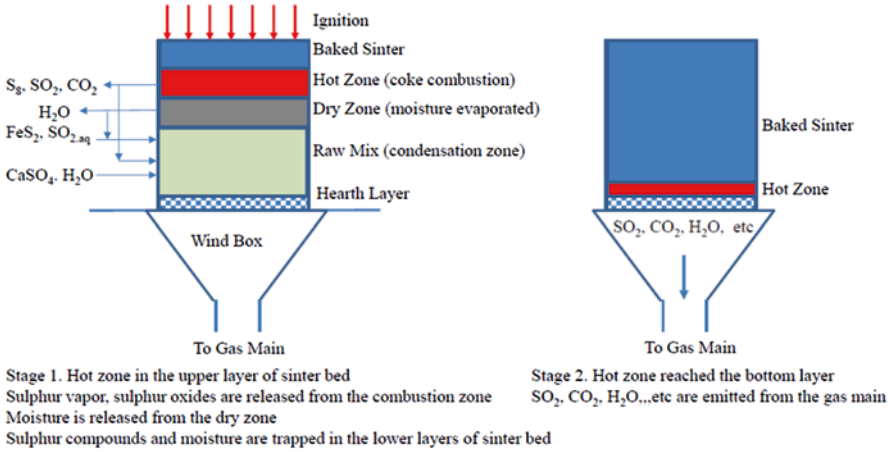

Fig. 5.6 SOx emission model for the iron ore sintering process

The unionized acid (H_2SO_3) has never been observed; the fraction of S(IV) in each species is a function of pH value. At pH < 2, $SO_{2(aq)}$ is dominant; pH at 2–8, HSO_3^- is formed; pH > 8, SO_3^{2-} is the preferred form.

A SOx emission model in sintering process is summarized as follows (Mou 1998). The sulfur released in the combustion stage is most likely to be absorbed and trapped below the dry zone. No matter whether the sulfur is liquid (S_8), sulfur dioxide (SO_2), or both, the sulfur is stored in several forms beneath the dry zone in the sintering process. When the combustion zone passes through the lower part of the sinter bed without any absorbent materials beneath it, the sulfur compounds oxidize to sulfur dioxide again and finally escape out to the atmosphere (Fig. 5.6).

5.3.5 Sulfur Journey in Iron Ore Sintering Process

Mou (1998) indicated that around 50–55 % of the sulfur in the sinter mix is from the coke breeze in the form of pyrite and organic sulfur; the other 45–50 % is from iron ores, fluxes, and reverts, mainly in the form of pyrite, chalcopyrite, and calcium sulfates. After heating, sulfur reacts with iron ores and limestone to form calcium sulfates and pyrite, which remain in the sinter. An estimated sulfur journey is summarized as follows (Mou 1998):

$$\text{Sulfur Raw Mix} = \text{Sinter} + \text{SP} / \text{RF} + \text{EP dust} + \text{Gases} \tag{5.2}$$

$$100\% = 18.9\% + 8.8\% + 1.1\% + 71.3\%$$

5.3.6 Conventional De-SOx Technologies

There are many applicable SOx removal technologies being applied in the combustion process. Most are off-gas treatment processes (Table 5.1). The side effects are the difficulties of resourcing these de-SOx by-products, especially the generated dust and sludge from the iron ore sintering process, which contain many impurities, such as iron ore powder, KCl, and NaCl. This causes a second pollution problem.

5.3.7 In-Process De-SOx Technology

Mou (1998) discovered an in-process de-SOx countermeasure by adding urea directly into the sinter mix. Urea decomposes to NH_3 at around 130 °C (Mcketta 1982) in the sinter bed dry zone and is trapped in the wet zone as NH_4OH and eventually released to the exhaust gas near the burnt through point (BTP), where the SOx (mainly SO_2) is also released out at the BTP, due to the strong affinity characteristic between NH_4SO_4 and SO_2. Eventually, $(NH_4)_2SO_4$, NH_4HSO_4, $(NH_4)_2SO_3$, and NH_4HSO_3 are formed inside the exhaust gas system. The SOx is converted to ammonium sulfates/sulfites/bisulfates/bisulfite, and therefore the SOx concentration in the outlet gases drops significantly.

Pot tests and plant trials have proven the de-SOx efficiency to 95 % (Mou 2001). The drawback is that the sticky $(NH_4)_2SO_4$ being brought out by the suction gas to the EP would adhere on the EP plate and wire and eventually lower the dust removal efficiency; the plume opacity becomes worse in a couple of days after the urea is added to the sintering process. Therefore, it is suggested to use wet EP or scrubber

Table 5.1 Conventional SOx removal processes

Process	Description	Reference
Active carbon absorption technology	SO_2 absorbed chemically or physically into the pores of active carbon	Slack (1975)
Metal oxide absorption technology	Metal oxides such as Mn, Fe, and Zn absorb SOx into sulfite or bisulfite at a lower temperature and desorb at a higher temperature	Slack (1975)
Lime base De-SOx technology	Limestone powder or hydrated lime reacts with SOx to form $CaSO_4 \cdot nH_2O$	Slack (1975)
Aqueous carbon process (ACP)	Sodium carbonate solution injected into the flue gases to form the sodium sulfite and/or sulfate to remove SOx	Slack (1975)
MgO De-SOx	$Mg(OH)_2$ injected into the flux gases to form $MgSO_4$(aq)	Burnett and Wells (1982)
Dry sorbent injection	Dry alkali sorbents injected into the flux gases to form the alkali sulfite or sulfate to remove SOx	Yet et al. (1982)

when urea is added. Actually, NH_3 is a basic reagent, besides its strong affinity to bind with SO_2 but also to bind with HCl. In other words, urea addition is capable of removing both SO_2 and HCl.

5.3.8 *Dioxins-PCDD/PCDF (Kasai 2002)*

Dioxins have been called the "century poison" with two congener groups being identified, polychlorinated dibenzo-p-dioxins (PCDD) and polychlorinated dibenzofurans (PCDF). In Japan, the coplanar polychlorinated biphenyls (Co-PCB) that have a similar toxicity are also treated as a subgroup of dioxins. The chemical structures of dioxins and their toxicity are shown in Fig. 5.7, and molecular structures are shown in Fig. 5.8.

Up to now, no conclusive evidence has been presented for the formation mechanism of PCDD/PCDFs. Two theories have been proposed, which are precursor condensation and de novo synthesis.

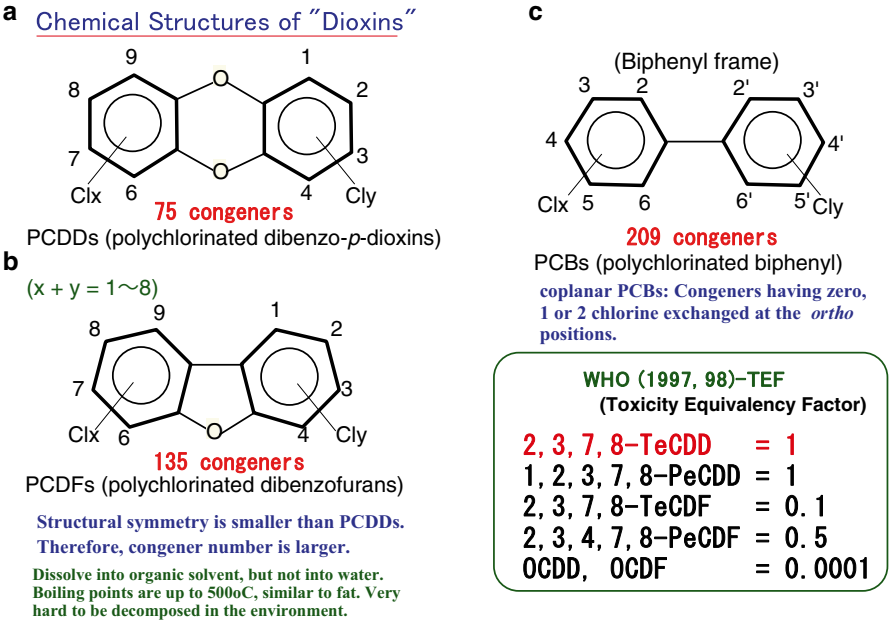

Fig. 5.7 Chemical structures of dioxins and their toxicities

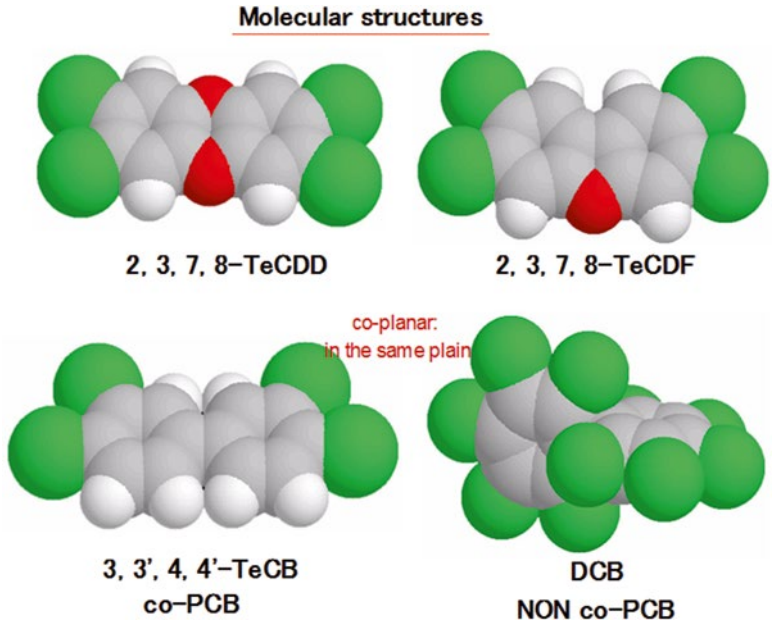

Fig. 5.8 Molecular structure of dioxins

5.3.9 Formation Mechanism of Dioxins (Kasai 2002)

1. Formation through precursors condensation
   Molecules with six-member ring structures, such as chlorobenzenes and chlorophenols, are heated in the combustion stage, where the chlorination, coupling reaction, and oxidation occur. Eventually, two six-member rings are joined together by two oxygen and the free radicals coupled with 1–8 Cl anions. The reaction temperature is above 800 °C, and the reaction is fast. The major congeners through precursors condensation are PCDDs. A schematic illustration of the precursor condensation route is shown in Fig. 5.9.
2. Formation through de novo synthesis
   Dioxins forming through de novo synthesis mean direct formation of dioxins from carbonaceous materials at relatively low temperature. Reactions to form dioxins involve the splitting of macromolecular compounds containing six-member rings. Normally, the reaction temperature is around 450 °C, and the major congeners are PCDF. An illustration of the de novo synthesis route is shown as Fig. 5.10.

Dioxin Formation in Sintering Process

Kasai (2002) established a dioxin formation model for the sintering process which explained the formation mechanism of dioxins in the sinter bed, as shown in Figs. 5.11 and 5.12.

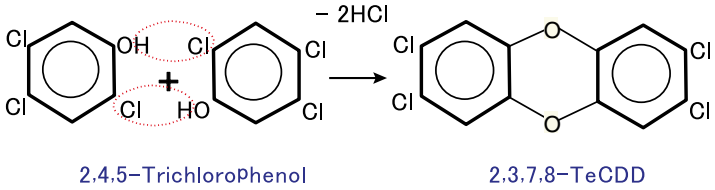

Fig. 5.9 Precursors condensation route for dioxin synthesis

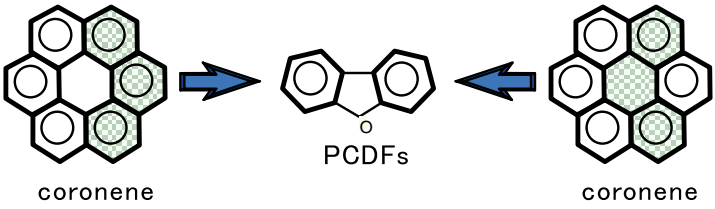

Fig. 5.10 De novo synthesis route for dioxin production

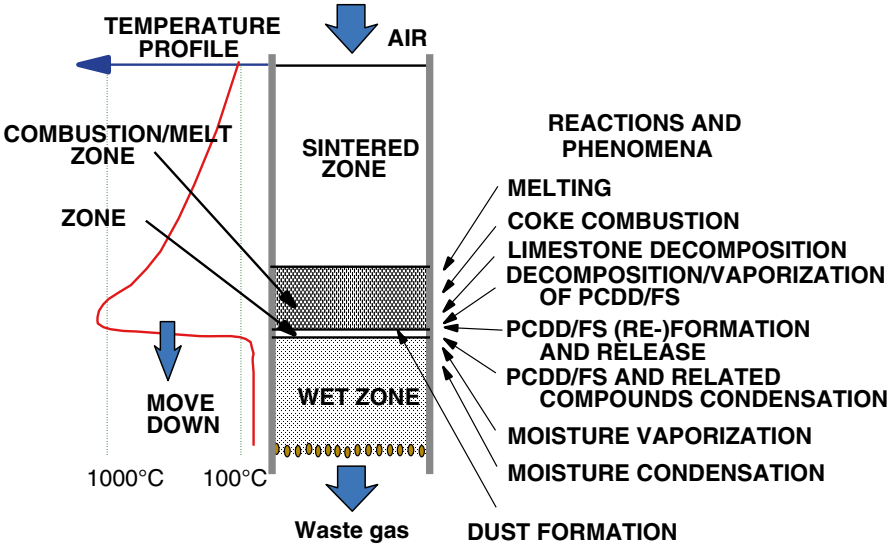

Fig. 5.11 Temperature profile and reaction zones in the sintering bed (Kasai, 2002)

Through the dioxin formation model, we can assume the dioxins would be released from the sinter bed when the combustion zone reaches the bottom; in other words, the dioxins are released out of the sinter bed around the BTP.

A survey result (Kasai 2002) indicated that the dioxin emission profile is similar to the temperature profile in each of the wind boxes. Additional surveys indicated that the major congeners of dioxins in the sintering process are PCDFs, the dominate congener is 23478-P5CDF, and the dominate congener for TEQ is 23478-P5CDF (Figs. 5.13 and 5.14).

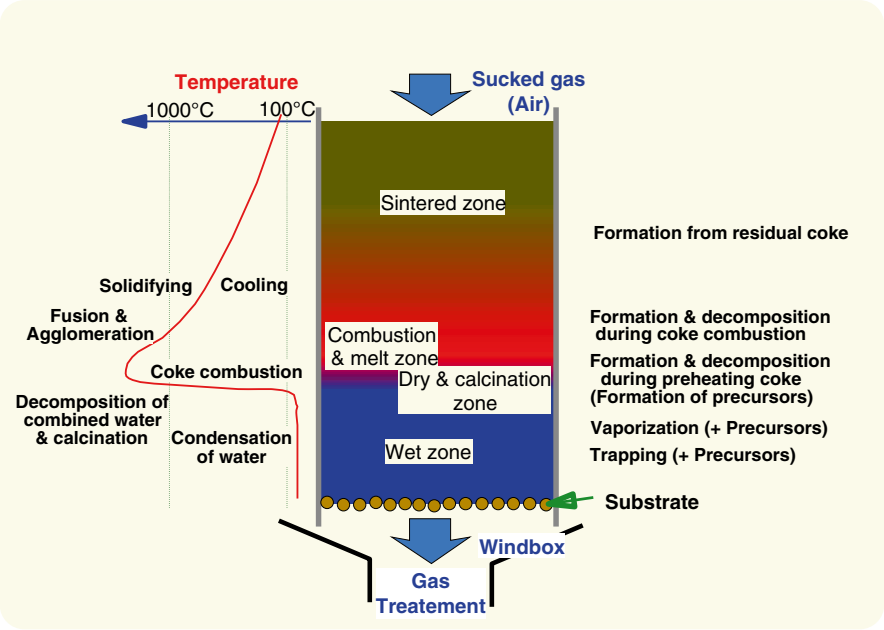

Fig. 5.12 Phenomena and reactions relating to the PCDD/PCDFs emission in the sintering bed PCDFs emission in the sintering (Kasai, 2002)

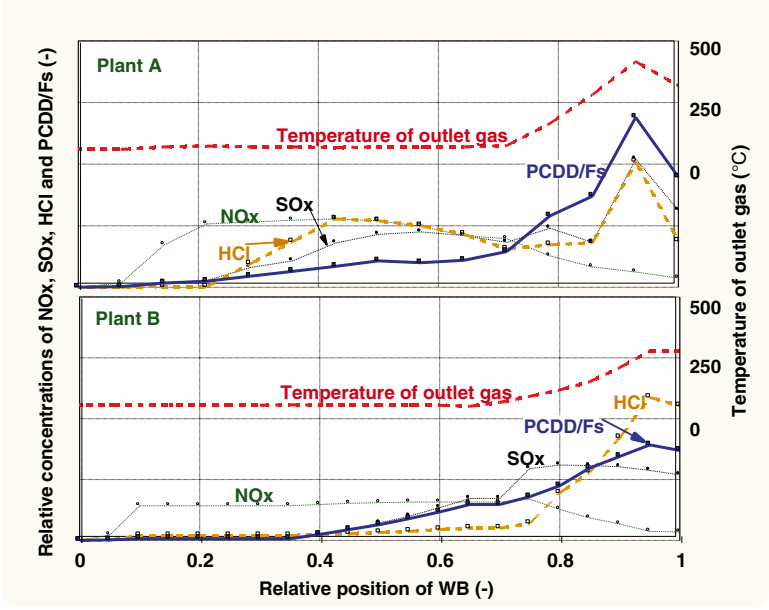

Fig. 5.13 Relative concentrations of PCDD/PCDFs and other gases in wind boxes with progress of sintering (Kasai, 2002)

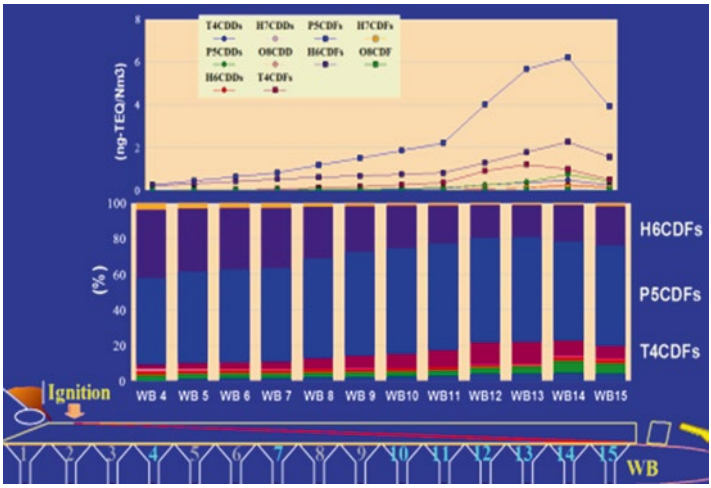

Fig. 5.14 Concentration and fraction of PCDD/PCDFs (TEQ) at the wind boxes of the sinter machine (Kasai, 2002)

Kasama et al. (2006) conducted a detailed analysis of the exhaust gas at the NSSMC Oita No. 1 sintering plant. This clarified and specified the strand positions where dioxins were released into the exhaust gas. The results are summarized as follows.

The release of dioxins was detected at two different positions. The first release position was located at the point where the drying zone reached the hearth layer, showing a broad peak containing a large amount of furans. The second release position was located at the point where the melting zone reached the heath layer, showing a sharp peak. Differences in dioxin congeners at the release positions imply a different mechanism of dioxin formation. The dioxins of the second release are considered to be formed in wind boxes at temperatures of 300 °C or more, with organic substances and chlorine supplied from incompletely sintered areas or with grease and dust in the wind boxes. This result has indicated that controlling the burn through point to the discharge end could be effective for decreasing the dioxin emissions in the second location. Figure 5.15 shows a schematic image describing the release of exhaust gas components.

Figure 5.15 also summarizes the results of the exhaust gas measurements in a commercial sinter plant. It seems that the drying zone begins to reach the grate surface near the sinter cake discharge side when the exhaust gas temperature reaches 100 °C. Thereafter, the exhaust gas temperature keeps on rising slowly, and the wet zone almost disappears within the subsequent strand as indicated by reading the moisture change. The dust ascends together with the dioxin ascent in the latter part, probably due to the loss of the capability of capturing them in the sintering bed as a result of the disappearance of the wet zone.

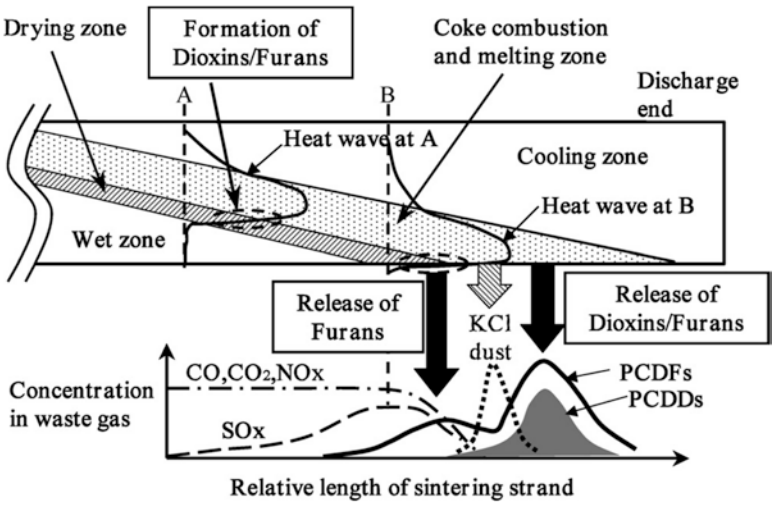

Fig. 5.15 Schematic image describing the release of exhaust gas components (Kasai, 2002)

From the results of the O_2, CO_2, and NOx measurements, the combustion of the fine coke seems to have been almost completed before it reached BTP. This may consequently indicate that, in the furthest area on the sinter cake discharge side after BTP, the coke combustion zone no longer exists and a high-temperature zone of over 1000 °C expands up to the hearth layer. Nevertheless, the wind box exhaust gas temperature rise is relatively slow because the sensible heat is consumed to increase the heat of the hearth layer and the grate.

From the next wind box, high-alkali and high-chlorine dust is affluently discharged. KCl and NaCl, which are considered to be the main components of the discharged dust, have a high melting point of 770 and 801 °C, respectively, and a high boiling point of 1510 and 1413 °C. In order to volatilize them, a condition near the highest temperature in the sintering bed is required. Therefore, the highest part of the sintering temperature must have reached up to the grate surface. This result agrees with the discussions of Kawaguchi et al. (2002) on the volatilization of chlorine. In BTP wind box, which comes after the chlorine release peak, a second-stage peak of dioxin release is observed. As regards the dioxins generated in the wind boxes close to the sinter cake discharge end, Tan and Neuschütz (2004) theoretically suggested the possibility of generation in the cooling process in the cooling zone, but no report has ever been made on this in commercial sintering equipment. The reason may be that, in production using sintering machines having a small number of wind boxes or in production where BTP is near the sinter cake discharge side, two phenomena occur in one wind box and these two could not be separately detected by the usual measurements.

The following two sources are conceivable for the supply of carbon and chlorine for the formation of dioxins in the second stage. One is the coke combustion zone that contains an un-sintered area where coke combustion remains incomplete until

it is discharged on account of sintering fluctuations. The incomplete combustion is often confirmed by the observation of sintered cakes on the discharge side. It is probable that small amounts of carbon and chlorine are supplied from this zone to cause dioxin formation such as the de novo synthesis reaction in the wind box. Although C and Cl are supplied in very small amounts, they are long exposed to a critical temperature zone, as long as several seconds, and may therefore be concentrated to a high level. The other source is grease and dust deposits on the inside surfaces of the wind boxes. Sealing grease is constantly fed to the slide surfaces of the sintering pallets. This grease loses its viscosity as it is heated in the latter half of the strand, is sucked into the wind box, and is deposited on its inside walls. Small amounts of chlorine contained in the grease and dust caught on the deposited grease are likely to cause dioxin generation slowly and progressively.

Kawaguchi et al. (2002) reported the memory effect of chlorine that remained in the wind box in their sinter pot test, seen in the form of re-volatilization and rediffusion of the chlorine in the drying process. Effects of said deposits in commercial operations need to be further analyzed in detail. Dioxins released in front of the BTP are reducible in quantity by strengthening the control of chlorine content or oil content in the raw materials for sintering, but different means of control are necessary for decreasing dioxins produced in the second stage. A practical effective means may be an appropriate control of the BTP position. There should be a control for setting a target BTP on the sinter cake discharge side within the tolerances of the operating conditions in terms of product yield, strength, exhaust gas temperature, etc. For high-productivity operation, BTP will be set on the utmost discharge side right from the start since the sintering rate cannot permit otherwise. For low-productivity operation, however, BTP may be set on the raw mixture feeding side of the strand as in the test being discussed. The operational results clearly show that the BTP position is varied on account of different factors and seem to indicate that holding the BTP stable on the discharge side can constrain dioxin release to a certain extent.

5.3.10 Countermeasures for Dioxin Reduction

5.3.10.1 Dioxin Reduction by SCR Catalyst

Mou (2005) conducted a pilot-scale test of dioxins reduction by using SCR catalysts in the No. 4 sinter plant of China Steel Corporation in year 2005. A test rig was installed adjacent to a sinter plant SCR de-NOx reactor (Fig. 5.16). Three types of catalysts had been tested: (1) plate-type $WO_3/V_2O_5/TiO_2$, (2) plate-type $MoO_3/V_2O_5/TiO_2$, and (3) honeycomb-type $(WO_3/V_2O_5/TiO_2)+(Pt/Al)$. The testing temperatures were set at 250, 290, 310, and 330 °C. The testing results are shown in Table 5.2 and summarized in the possible mechanism as follows:

1. Dioxin reduction efficiency reduced as the operational temperature increased.
2. The test results showed the reduction efficiency is around ~28 to ~45 %. The three types of catalyst removal efficiencies were all similar.

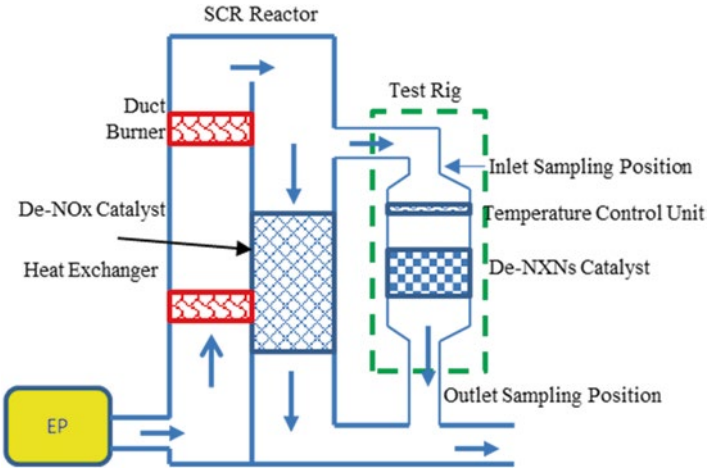

Fig. 5.16 SCR catalyst test rig for dioxin removal

Table 5.2 Toxicity removal efficiency (%) of SCR catalysts at different operational temperatures

°C	330	310	290	250
$WO_3/V_2O_5/TiO_2$	22.7	40.2	42.9	
$MoO_3/V_2O_5/TiO_2$	32.8	30.8	38.5	46.6
$(WO_3/V_2O_5/TiO_2) + (Pd/Al)$	29.1	27.5	36.8	44.4

3. The gas phase dioxin removal efficiency was higher than the solid phase.
4. During tests where dust accumulation on the catalyst surface was observed, these dusts contained rich KCl (source for Cl), unburnt coke breeze fines (source for C), and Fe_2O_3 (de novo catalyst); moreover, the SCR operation temperature is around 300–350 °C; hence, the surface of catalysts provided a suitable de novo synthesis environment. It was therefore assumed that dioxins formed on the surface of catalyst as the temperature stepped into the reaction window.
5. The removal efficiency of low chlorine (4, 5) dioxins was higher than high chlorine (6–8) dioxins. The removal efficiency of PCDD was higher than PCDF.
6. Sampling data showed the toxicity of PCDF was about 10 times that of PCDD.

5.3.10.2 Dioxin Removal by Lignite Coke Absorption

Mou and Passler (2008) conducted a demonstration scale test of lignite pack bed filter for dioxin removal in China Steel No. 2 sinter plant. The filter bed system is equipped with a long tube container with the $L \times W \times H = 6.05 \times 2.43 \times 2.90$ m^3. It

was a module design with the gas treating capability of 60,000 m^3 gas per hr per unit, and it could be connected in parallel in different units according to the required gas handling amount. The reason for choosing lignite coke was the pore diameter more suitable to trap the dioxin molecules than active carbon, and it also was more noncombustible than active carbon.

The basic concept was to deploy the lignite coke on top of an inclined screen net for around 10 cm; waste gases passing through the packed bed and those dioxins, submicron particles, alkali chlorides, sulfates, etc. were trapped on/in the packed bed. Purging air was introduced for backwashing when the pressure drop reached a certain level due to caking on the pack bed; this caking together with upper layer lignite coke was removed by screw discharger, and the fresh lignite coke continues to supplement on the pack bed. Figures 5.17, 5.18, 5.19, and 5.20 show the working principle of the filter bed.

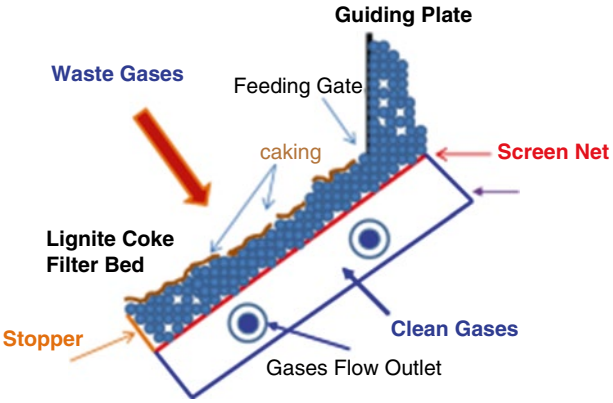

Fig. 5.17 Operation in gas purification stage

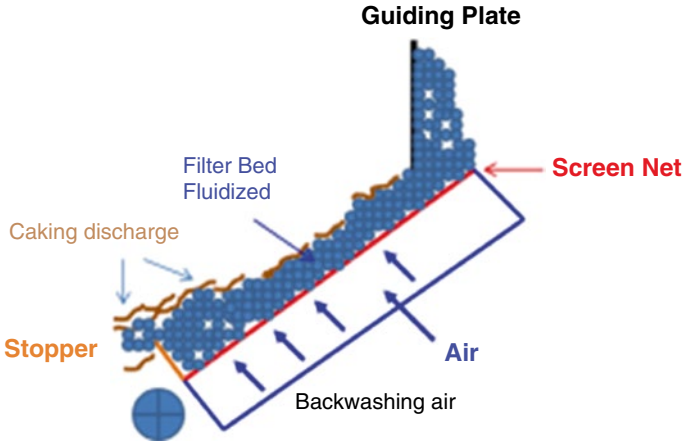

Fig. 5.18 Operation in air back washing stage

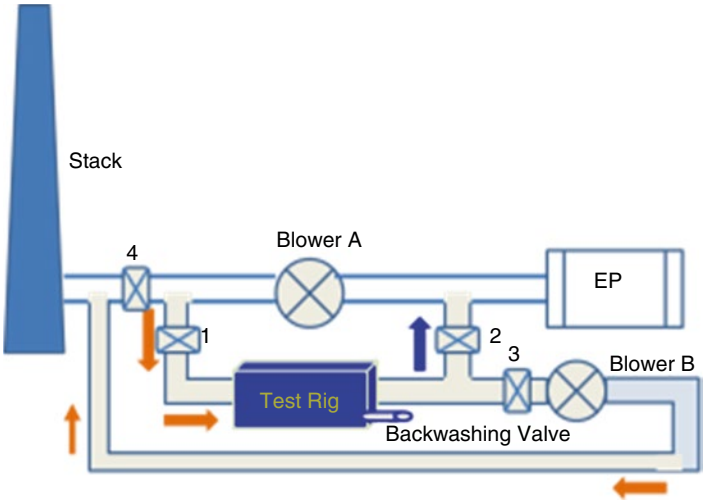

Fig. 5.19 Operational loop for testing module

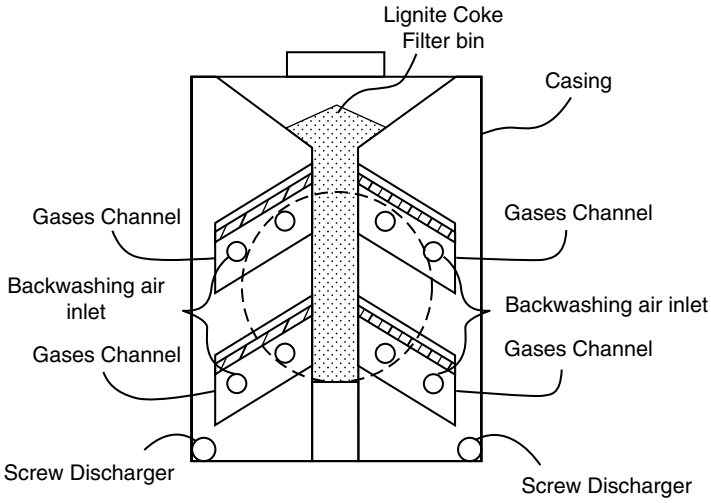

Fig. 5.20 Cross section of pack bed filter

Table 5.3 Average data for lignite pack bed testing results

	Filter Wt (B)	Filter Wt (A)	Sampling V (Nm^3)	Dust (mg/Nm^3)	O_2 (%)	O_2 corrected (ng I-TEQ/Nm^3)					
						Gas	Gas removal%	Solid	Sol removal%	Total	Removal%
In	0.338	0.359	1.761	12.054	15.37	1.028	NA	0.159	NA	1.289	NA
Out	0.559	0.563	2.106	2.342	14.44	0.017	98.3	0.013	92.1	0.029	97.7

For 3-month continuous testing, dioxin average removal efficiency reached around 98 % (Table 5.3). It is believed that the filter bed device is a potential apparatus for dioxins, submicron particle, and acid gas removal.

References

Anderson DC, Galwey AK (1995) Surface texture changes during reaction of $CaCO_3$ crystals with SO_2 and O_2, Air 3. In presence of coal combustion, 870–920 K. Fuel 74:101–1035

Burnett TA, Wells WL (1982) Conceptual design and economics of an improved magnesium oxide flue gas desulfurization process. In: Flue gas de-sulfurization, Chapter 18. American Chemical Society, pp 381–411

Glassman I (1987) Combustion, 2nd edn. Academic, New York, pp 318–361

Hida Y, Sasaki M, Ito K (1980) Consideration on CO and NO formation around the coke specimen during combustion. Tetsu-to-Hagane 66(13):21–29

Kasai E, Wu S, Sugiyama T, Inaba S, Omori Y (1992) Combustion rate and NO formation during combustion of coke granules in packed beds 1. Tetsu-to-Hagane 78(7):51–57

Kasai E, Wu S, Sugiyama T, Omori Y, Inaba S (1993a) Emission of nitrogen oxides during combustion of coke granules in packed beds. In: The third world conference on experimental heat transfer, fluid mechanism and thermodynamic, Honolulu, Hawaii, USA, Elsevier Science Publishers B.V., 31 Oct. to 5 Nov. 1993, pp 1065–1072

Kasai E, Sakata M, Sugiyama T, Omori Y, Yoshikawa O, Inaba S (1993b) Emission of nitrogen oxides and other nitrogen oxides from iron ore sintering process. In: Proceedings of sixth international symposium on agglomeration, Nagoya, Japan, pp 375–339

Kasai E (2002) Introduction of dioxins forming mechanism and their abatement countermeasures, presentation and discussions in China Steel Corporation, Kaoshiung, 2–5 July 2002

Kasama S, Yamamura Y, Watanabe K (2006) Investigation on the dioxin emissions from a commercial sintering plant. ISIJ Int 46(7):1014–1019

Kawaguchi T, Matsumura M, Hosotani Y, Kasai E (2002) Behavior of trace chlorine in sintering bed and its effect on dioxins concentration in exhaust gas of iron ore sintering. Tetsu-to-Hagané 88:59

Martin LR (1984) Kinetic studies of sulphur oxidation in aqueous solution, Chapter 2, SO_2, NO and NO_2 Oxidation Mechanism, Atmosphere Consideration. Jack G. Calvert, USA

Mcketta JJ (1982) Encyclopedia of chemical processing and design, vol 8, fertilizer components: ammonium sulfate. Marcel Dekker Inc., New York and Basel, pp 273–283

Mou JL (1992) A survey of the influence of sinter raw materials on NOx, SOx emission. TE-81023, Internal Technical Report of China Steel Corporation, Taiwan

Mou JL (1998) A study of in-plant De-NOx and De-SOx in the iron ore sintering process. PhD Thesis, Environmental Science Department, University of Wollongong, Australia

Mou JL (2001) In-plant reduction of NOx, SOx emission in iron ore sintering process, China Steel Technical Report No. 15, 31–36, Dec. 2001, Taiwan

Mou JL (2005) Evaluation of SCR catalysts for dioxins removal-pilot test, ST-94025, China Steel Corp. Internal Research Report

Mou JL, Passler K (2008) Report on NDF Demo Unit in CSC No. 2 SP. China Steel Corporation Taiwan

Pimenta FV (2012) Sintering process. Vale Training Course for Formosa Ha-Tinh Steel Corporation

Sasaki M, Hida Y, Enokio T, Ito K (1990a) The relationship between coke existing state and NO formation. Tetsu-to-Hagané 76:S57

Sasaki M, Hida Y, Enokio T, Ito K (1990b) A study of fuel NO formation and depression. Tetsu-to-Hagané 76:S58

Slack AV (1975) Sulfur dioxide removal from waste gases, 2nd edn. Noyes Data Corp., Park Ridge

Suzuki G, Ando R, Yoshikoshi H, Yamaoka Y, Nagaoka S (1975) A study of the reduction of NOx in the waste gas from sinter plants. Tetsu-to-Hagane 61, 3–13

Tan P, Neuschütz D (2004) Metall Mater Trans B 35B:983–991. doi:10.1007/s11663-004-0092-7
Tu LC, Liu GC (1992) A survey report of iron ore sinter plant De-NOx facilities. Engineering and Construction Dept. (V23), Internal Technical Report of China Steel Corporation, Taiwan
Vegman EF, Zherebin BN, Pochvisnev AN, Yusfin YuS, Kurunov IF, Parenkov AE, Chernousov PI (2004) Ironmaking. Akademkniga, Moscow, p 774
Wright J (2014) Review of human health risks – emissions from sinter plant. Principal/Director Environmental Risk Sciences Pty Ltd. Wollongong, Australia
Yet JT, Demski RJ, Joubert JI (1982) Control of SO_2 emission by dry sorbent injection. Chapter 16. In: Flue gas desulfurization. American Chemical Society, USA, pp 349–367